Journal Pre-proof

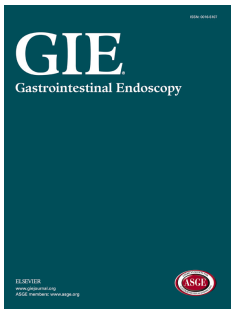

Establishment of a patient-specific avatar organoid model derived from endoscopic ultrasonography-guided fine needle biopsy for timely clinical application in pancreatic ductal adenocarcinoma

Hyemin Kim, Ph.D, Jinho Jang, Ph.D, Jin Ho Choi, MD, Ph.D, Joo Hye Song, MD, Ph.D, Su Hyun Lee, BS, Jiho Park, Ph.D, Si Kyong Ryoo, MD, Eun Mi Lee, MS, Hyoung-oh Jeong, Ph.D, Seunghoon Kim, BS, Se-Hoon Lee, MD, Ph.D, Kwang Hyuck Lee, MD, Ph.D, Kyu Taek Lee, MD, Ph.D, Kyoung Mee Kim, MD, Ph.D, Kee-Taek Jang, MD, Ph.D, Hyunsook Lee, Ph.D, Semin Lee, Ph.D, Jong Kyun Lee, MD, Ph.D, Joo Kyung Park, MD, Ph.D

PII: S0016-5107(24)00132-9

DOI: https://doi.org/10.1016/j.gie.2024.02.021

Reference: YMGE 14169

To appear in: *Gastrointestinal Endoscopy*

Received Date: 29 October 2023

Revised Date: 16 February 2024

Accepted Date: 19 February 2024

Please cite this article as: Kim H, Jang J, Choi JH, Song JH, Lee SH, Park J, Ryoo SK, Lee EM, Jeong H-o, Kim S, Lee S-H, Lee KH, Lee KT, Kim KM, Jang K-T, Lee H, Lee S, Lee JK, Park JK, Establishment of a patient-specific avatar organoid model derived from endoscopic ultrasonography-guided fine needle biopsy for timely clinical application in pancreatic ductal adenocarcinoma, *Gastrointestinal Endoscopy* (2024), doi: https://doi.org/10.1016/j.gie.2024.02.021.

Establishment of a patient-specific avatar organoid model derived from endoscopic ultrasonography-guided fine needle biopsy for timely clinical application in pancreatic ductal adenocarcinoma

Hyemin Kim, Ph.D[1*], Jinho Jang, Ph.D[2*], Jin Ho Choi, MD, Ph.D[1*], Joo Hye Song, MD, Ph.D[1*], Su Hyun Lee, BS[3], Jiho Park, Ph.D[3], Si Kyong Ryoo, MD[1], Eun Mi Lee, MS[1], Hyoung-oh Jeong, Ph.D[2], Seunghoon Kim, BS[2], Se-Hoon Lee, MD, Ph.D[1,4], Kwang Hyuck Lee, MD, Ph.D[1], Kyu Taek Lee, MD, Ph.D[1], Kyoung Mee Kim, MD, Ph.D[5], Kee-Taek Jang, MD, Ph.D[5], **Hyunsook Lee, Ph.D[3†], Semin Lee, Ph.D[2†], Jong Kyun Lee, MD, Ph.D[1†], and Joo Kyung Park ,MD, Ph.D[1,4†]**

[1]Department of Medicine, Samsung Medical Center, Sungkyunkwan University School of Medicine, Seoul, Korea.

[2]Department of Biomedical Engineering, School of Life Sciences, Ulsan National Institute of Science and Technology, Ulsan, Korea.

[3]Department of Biological Sciences, Institute of Molecular Biology and Genetics, Seoul National University, Seoul, Korea.

[4]Department of Health Sciences and Technology, SAIHST, Sungkyunkwan University, Seoul, Republic of Korea

[5]Department of Pathology, Samsung Medical Center, Sungkyunkwan University School of Medicine, Seoul, Korea.

*These authors contributed equally to this study.

Correspondence

Joo Kyung Park, M.D., Ph.D.

Department of Medicine, Samsung Medical Center, Sungkyunkwan University School of Medicine, 81 Irwon-ro, Gangnam-gu, Seoul, 06351, Republic of Korea.

Tel: +82-2-3410-3409, Fax: +82-2-3410-6983, E-mail: jksophie.park@samsung.com

Semin Lee, Ph.D.

Department of Biomedical Engineering, Ulsan National Institute of Science and Technology (UNIST), 50 UNIST-gil, Ulsan, 44919, Republic of Korea.

Tel: +82-52-217-2663, Fax: +82-52-217-3582, E-mail: seminlee@unist.ac.kr

Hyunsook Lee, Ph.D.

Department of Biological Sciences, Institute of Molecular Biology and Genetics, Seoul National University, 1 Gwanak-Ro, Gwanak-Gu, Seoul, 08826, Republic of Korea.

Tel: +82-2-886-4339, Fax: +82-2-886-4335, E-mail: hl212@snu.ac.kr

Jong Kyun Lee, M.D., Ph.D.

Department of Medicine, Samsung Medical Center, Sungkyunkwan University School of Medicine, 81 Irwon-ro, Gangnam-gu, Seoul, 06351, Republic of Korea.

Tel: +82-2-3410-3409, Fax: +82-2-3410-6983, E-mail: jongk.lee@samsung.com

Author contributions

HK - analysis and interpretation of the data, drafting of the article, critical revision of the article for important intellectual content; JJ - analysis and interpretation of the data, drafting of the article; JHC - drafting of the article, critical revision of the article for important intellectual content; JHS- analysis and interpretation of the data, drafting of the article; SHL, JP, SKR, EML, H-OJ and SK - analysis and interpretation of the data; S-HL, KHL, KTL, KMK, and K-TJ - conception and design; HL, SL, JKL, and JKP - conception and design, final approval of the article. All authors read and approved the final manuscript.

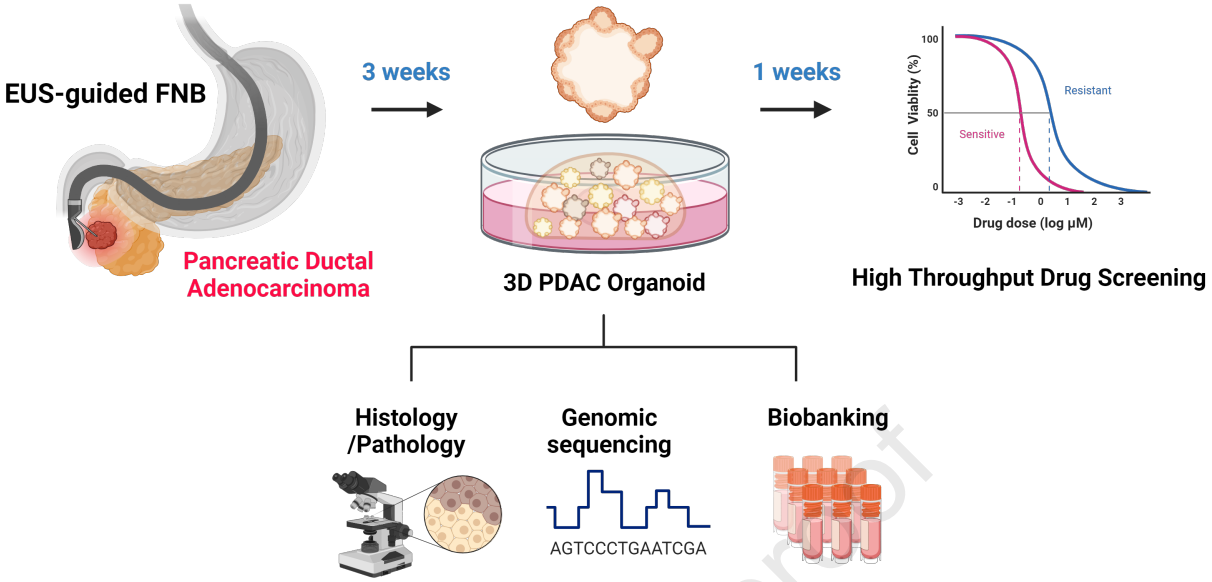

Establishment of a patient-specific avatar organoid model derived from endoscopic ultrasonography-guided fine needle biopsy for timely clinical application in pancreatic ductal adenocarcinoma

Hyemin Kim, Ph.D[1*], Jinho Jang, Ph.D[2*], Jin Ho Choi, MD, Ph.D[1*], Joo Hye Song, MD, Ph.D[1*], Su Hyun Lee, BS[3], Jiho Park, Ph.D[3], Si Kyong Ryoo, MD[1], Eun Mi Lee, MS[1], Hyoung-oh Jeong, Ph.D[2], Seunghoon Kim, BS[2], Se-Hoon Lee, MD, Ph.D[1,4], Kwang Hyuck Lee, MD, Ph.D[1], Kyu Taek Lee, MD, Ph.D[1], Kyoung Mee Kim, MD, Ph.D[5], Kee-Taek Jang, MD, Ph.D[5], **Hyunsook Lee, Ph.D[3†], Semin Lee, Ph.D[2†], Jong Kyun Lee, MD, Ph.D[1†], and Joo Kyung Park ,MD, Ph.D[1,4†]**

[1]Department of Medicine, Samsung Medical Center, Sungkyunkwan University School of Medicine, Seoul, Korea.

[2]Department of Biomedical Engineering, School of Life Sciences, Ulsan National Institute of Science and Technology, Ulsan, Korea.

[3]Department of Biological Sciences, Institute of Molecular Biology and Genetics, Seoul National University, Seoul, Korea.

[4]Department of Health Sciences and Technology, SAIHST, Sungkyunkwan University, Seoul, Republic of Korea

[5]Department of Pathology, Samsung Medical Center, Sungkyunkwan University School of Medicine, Seoul, Korea.

*These authors contributed equally to this study.

Correspondence

Joo Kyung Park, M.D., Ph.D.

Department of Medicine, Samsung Medical Center, Sungkyunkwan University School of Medicine, 81 Irwon-ro, Gangnam-gu, Seoul, 06351, Republic of Korea.

Tel: +82-2-3410-3409, Fax: +82-2-3410-6983, E-mail: jksophie.park@samsung.com

Semin Lee, Ph.D.

Department of Biomedical Engineering, Ulsan National Institute of Science and Technology (UNIST), 50 UNIST-gil, Ulsan, 44919, Republic of Korea.

Tel: +82-52-217-2663, Fax: +82-52-217-3582, E-mail: seminlee@unist.ac.kr

Hyunsook Lee, Ph.D.

Department of Biological Sciences, Institute of Molecular Biology and Genetics, Seoul National University, 1 Gwanak-Ro, Gwanak-Gu, Seoul, 08826, Republic of Korea.

Tel: +82-2-886-4339, Fax: +82-2-886-4335, E-mail: hl212@snu.ac.kr

Jong Kyun Lee, M.D., Ph.D.

Department of Medicine, Samsung Medical Center, Sungkyunkwan University School of Medicine, 81 Irwon-ro, Gangnam-gu, Seoul, 06351, Republic of Korea.

Tel: +82-2-3410-3409, Fax: +82-2-3410-6983, E-mail: jongk.lee@samsung.com

Abstract

Background and aims: Pancreatic ductal adenocarcinoma (PDAC) has the worst survival rate among tumors. At the time of diagnosis, over 80 percent of PDACs are considered surgically unresectable, and there is an unmet need for treatment options in these inoperable PDACs. The study aimed to establish a patient-derived organoid (PDO) platform from endoscopic ultrasound-guided fine needle biopsy (EUS-FNB) collected at diagnosis and to determine its clinical applicability for the timely treatment of unresectable PDAC.

Methods: Patients with suspected PDAC were prospectively enrolled at the Samsung Medical Center from 2015 to 2019. PDAC tissues were acquired by EUS-FNB to establish PDAC PDOs, which were comprehensively analyzed for histology, genomic sequencing, and high-throughput screening (HTS) drug sensitivity test.

Results: PDAC PDOs were established with a success rate of 83.2% (94/113). It took approximately 3 weeks from acquiring minimal EUS-FNB specimens to generating sufficient PDAC PDOs for the simultaneous analysis of HTS drug sensitivity test and genomic analysis. The high concordance between PDAC tissues and matched PDOs was confirmed, and whole-exome sequencing revealed the increased detection of genetic alterations in PDOs, compared with in EUS-FNB tissues. The HTS drug sensitivity test showed the clinical correlation between the *ex vivo* PDO response and the actual chemotherapeutic response of the study patients in the real world (13 out of 15 cases). In addition, whole-transcriptome sequencing identified candidate genes associated with nab-paclitaxel resistance, such as *ITGB7*, *ANPEP,* and *ST3GAL1*.

Conclusions: This PDAC PDO platform allows several therapeutic drugs to be tested within a short time window and opens the possibility for timely personalized medicine as a “Patient Avatar Model” in clinical practice.

Keywords: pancreatic ductal adenocarcinoma (PDAC), endoscopic ultrasound-guided fine needle biopsy (EUS-FNB), patient-derived organoid (PDO), high-throughput screening (HTS) drug sensitivity test, personalized medicine.

Introduction

Pancreatic ductal adenocarcinoma (PDAC) is one of the most lethal solid malignancies; the 5-year relative survival rate is the lowest (9%) among cancers, and while the death rate has risen over the past decade (1, 2). PDAC is mainly treated with a combination of cytotoxic chemotherapeutic agents, gemcitabine and nab-paclitaxel (GnP) or FOLFIRINOX (5-fluorouracil, leucovorin, irinotecan, and oxaliplatin) combined with surgery, but at the time of diagnosis, less than 20 % of PDACs are resectable (3-5).

Recently, a patient-derived organoid (PDO) was developed, and upon embedding in a three-dimensional (3D) matrix, could be grown with high efficiency into a self-organizing organotypic structure. Tumor organoids can remain genetically and phenotypically stable with long-term expansion, leading to a wide range of applications in cancer research for drug development and personalized medicine (6, 7). However, the role that PDO models play in clinical practice as avatars for PDAC patients has never been fully proven; they have not been applied in actual practice due to certain general barriers related to cancer organoids, which include lack of a consistent standard protocol, excessively long time for establishment, and difficulty in obtaining pure cancer organoids (8).

Even though most PDACs are inoperable at the time of diagnosis, most PDO models use surgical specimens from resectable tumors, while some PDO models use endoscopic ultrasound-guided fine needle biopsy (EUS-FNB) specimens of unresectable PDACs (9-12). Since biopsy is the current gold standard for diagnosing PDACs, biopsy acquisition from patients with unresectable PDACs can be a useful technique. Furthermore, surgical specimens are usually acquired after portal vein

117 dissection and vascular clamping, which automatically cause ischemic damage and
118 the autolysis of pancreatic cells. However, the EUS-FNB technique enables relatively
119 undamaged and fresh tissue to be acquired under the normal physiologic state of the
120 patient, leading to a higher rate of successful establishment of PDAC PDOs (13).

121 Therefore, the aims of this study were 1) to establish a PDAC PDO platform
122 using minimal EUS-FNB specimens from unresectable PDAC patients for timely
123 clinical assessment with high efficacy, 2) to investigate clinicopathologic and genomic
124 characteristics, and 3) to determine the clinical applicability of the PDAC PDO model
125 as a patient avatar for predicting treatment response and prognosis.

126

127 Methods

128 Study Patients

129 Patients with suspected unresectable PDAC were prospectively enrolled in the
130 Samsung Medical Center (SMC) between June 2015 and October 2019. All patients
131 provided written informed consent, and all specimens were collected according to
132 Institutional Review Board (IRB) regulations and approval (IRB No. 2014-04-061,
133 2016-05-011). The clinical features and laboratory data were collected using electronic
134 medical records. In addition, tumor size, metastatic site, treatment course, and
135 response to treatment followed the RECIST guideline (RECIST v1.1). In examining
136 the concordance between palliative chemotherapy outcomes and drug responses in
137 PDAC PDOs, we focused on analyzing the best responses as defined by RECIST v1.1,
138 coupled with a review of survival durations.

139 Endoscopic ultrasound-guided fine needle biopsy (EUS-FNB)

140 All EUS-FNB was performed under conscious sedation by the same

141 experienced endosonographer (JKP) using a standard curvilinear array
142 echoendoscope (GF-UE160-AL linear EUS apparatus, Olympus) equipped with an
143 Aloka ProSound SSD 5000 processor (Wallingford) and 22-gauge Acquire® FNB
144 needle (Boston Scientific). Each needle throw was fanned about the entire mass area
145 to obtain the best representative sample. The obtained EUS-FNB specimens were
146 placed into MACS® Tissue storage solution (Miltenyi Biotec.) and immediately further
147 processed.

148 **Patient-Derived Organoids (PDOs)**

149 We cultivated organoids using patient-derived PDAC tissue acquired from the
150 EUS-FNB. Tumors were homogenized with GentleMACS™ tissue dissociator and
151 human tumor dissociation kit (Miltenyi Biotec.). Isolated cells were plated with Matrigel
152 (Corning) and complete media (Supplementary Table 1). Generated PDOs were
153 further applied for banking, immunostaining, genomic analysis, and drug screening for
154 clinical response evaluation (Supplementary Fig. 1). For histological validation,
155 formalin-fixed PDOs were incubated with antibodies (Supplementary Table 2) at 4°C
156 overnight. After counterstaining with DAPI, immunofluorescent images were observed
157 and captured by an LSM780 confocal microscope system (ZEISS).

158 **High-Throughput Screening (HTS) Drug sensitivity test**

159 Using an HTS platform first reported in October 2018 (14), we were able to test
160 twenty PDOs in a non-stop workflow from EUS-FNB to HTS drug sensitivity test
161 without biobanking. PDOs were dissociated into single cells and seeded on 384-well
162 plates (500 cells/well) with technical duplicates. Cells were treated with 71 kinds of
163 drugs targeting major oncogenic pathways in 4-fold and 7-point serial dilutions. After
164 7-day treatment, cell viability was assessed using an adenosine triphosphate (ATP)

monitoring system based on firefly luciferase (ATPlite 1step) and estimated by EnVision Multilabel Reader (PerkinElmer). The relative viability for each dose was obtained by normalization with dimethyl sulfoxide per plate. Dose–response curves (DRCs) were fitted using GraphPad Prism 8.0 (GraphPad Software Inc.). The area under the curve (AUC) for each DRC was calculated, and the value of the normalized AUC was obtained by dividing the AUC value by the maximum area for the concentration range measured.

Whole-Exome Sequencing (WES) and Whole-Transcriptome Sequencing (WTS)

We performed WES and WTS for PDAC PDOs that also subjected to HTS drug sensitivity test. For WES, genomic DNA was subjected to Agilent Sure-Select Human All Exon v6 and sequenced by the Illumina HiSeq4000 platform. Burrows–Wheeler aligner (15) for read alignment to the human reference genome (GRch37), MuTect2 (16) for the detection of somatic single nucleotide variations (SNVs) and short insertions and deletions (indels), control-FREEC (17) for the identification of somatic copy number alterations (SCNAs) and Sequenza (18) for the estimation of the ploidy and cellularity of EUS-FNB tissues and PDOs were used. For WTS, Mapsplice for read alignment to the human reference genome and transcriptome (build GRCh37), DESeq2 (19) for the identification of differentially expressed genes (DEGs), and Enrichr R package (20, 21) for the gene set enrichment test (GSEA) with the Kyoto Encyclopedia of Genes and Genomes (KEGG) pathway database were used.

Statistical analysis

Differences between continuous variables were analyzed using unpaired Student's *t* test, while differences between categorical variables were analyzed using the χ^2 test and Fisher's exact test as appropriate. Logistic regression analysis

identified independent factors associated with the success of PDO establishment. The gene expression data and clinical information for the PDAC cohort from The Cancer Genome Atlas (TCGA) were downloaded from GDAC (https://gdac.broadinstitute.org/). The upper and lower 33 % percentiles of expression were used to determine the high and low groups, and the survival curve was analyzed by the Kaplan–Meier method. A *P* value <0.05 was considered to indicate statistical significance. All statistical analyses were performed using SPSS software version 27.0 for Windows (SPSS) or GraphPad Prism 8.0 (GraphPad Software).

Results

Establishment of PDAC PDOs from minimal EUS-FNB specimens with high success rate

A total of 113 newly diagnosed PDAC patients were finally enrolled, and Table 1 summarizes the baseline characteristics. The median age was 65 years, and males were 57.5%. The distribution of stage (8th AJCC) was as follows: stage IA/IB 14 (12.4%); stage IIA/IIB 7 (6.2%); stage III 33 (29.2%); and stage IV 59 (52.2%). A total of 90 patients (79.6%) were treated with palliative chemotherapy. Finally, ninety-four PDAC PDOs were established from 113 EUS-FNB specimens with a success rate of 83.2% (Supplementary Fig. 2). We also analyzed clinical factors associated with the success of PDO establishment (Table 1). Determination of whether PDO generation was successful or not found no significant difference. Multivariable analysis found that specimens with high cellularity (>10 clusters) generated PDAC PDOs with higher efficiency (*P*=0.044) than those with mild cellularity (<3 clusters). PDAC patients with successful organoid growth did not show a significant difference in overall survival

213 (OS), compared to patients with failed organoid growth (Supplementary Fig. 3,
214 *P*=0.636), despite suspicious aggressive tumor biology in PDAC patients with shorter
215 OS.

216 **Histological and genomic validation of the PDAC PDOs**

217 The PDAC PDOs exhibited various morphologies, such as hollow structures,
218 densely packed spheres, and irregular architecture (Supplementary Video and
219 Supplementary Fig. 4). Hematoxylin & Eosin staining showed that PDOs had
220 morphological features similar to those of patient tissues (Fig.1A). PDAC PDOs were
221 also verified by immunofluorescence staining for epithelial tumor markers cytokeratin
222 (CK) and EpCAM (22, 23), ductal cell markers DBA-lectin and SOX9 (24, 25), PDAC
223 marker Plectin-1 (26), and PDAC stem cell marker CD133 (27). Phalloidin and DAPI
224 were used to confirm the cytoskeleton (F-actin) and nucleus, respectively (Fig. 1B).

225 To confirm whether PDAC PDOs can well represent the genomic
226 characteristics of the original PDACs, whole-exome sequencing (WES) was
227 performed to identify SCNAs with EUS-FNB specimens, matched PDOs, and matched
228 blood. In Fig. 1C, the cellularity of each sample showed the clonal homogeneity of
229 PDOs derived from the heterogeneous FNBs. Nine (Pt.2, Pt.4, Pt.5, Pt.8, Pt.9, Pt.11,
230 Pt.13, Pt.14, and Pt.15) out of 13 cases (69 %) showed higher cellularity in PDOs than
231 in matched FNBs, suggesting the development of unique clones. Additionally, we
232 found positively correlated SCNA profiles between FNBs and PDOs (average
233 Pearson's correlation coefficient: 0.75), confirming their genomic concordance. WES
234 analysis identified several recurrently mutated genes in FNBs and PDOs by somatic
235 SNVs and indels. Protein sequence-altering somatic point mutation profiles were
236 similar between FNBs and matched PDOs, suggesting the concordance of genomic

profiles (Fig. 1D). Importantly, several key mutations, such as *KRAS*, *TP53*, *KMT2D,* and *RNF43,* were more frequently detected in PDAC PDOs than FNBs, which indicates the high quality of genomic analysis in PDOs. The frequency of mutations in *KRAS,* the most frequently mutated oncogene in PDAC (28-30), was higher in PDOs (92 %) than in FNBs (67 %). These results represent that PDAC PDOs have concordance with the matched EUS-FNB samples and show higher purity of tumor cells for genomic characterization and subsequent analyses, such as drug screening.

Landscape of the Drug Sensitivity in PDAC PDOs

Next, high-throughput screening (HTS) drug sensitivity test was performed for twenty well-established PDAC PDOs. It took about 21 days (median, ranging 13-43 days) from taking minimal EUS-FNBs to generating enough PDOs for the simultaneous analysis of HTS test, histological staining, genomic sequencing and biobanking. At that time, PDOs were 3 passages of cultures (median, ranging 2-6 passages). PDAC PDOs were treated with 71 kinds of drugs for 7 days and the drug panel included 1) standard cytotoxic chemotherapeutic agents for PDAC, such as gemcitabine, nab-paclitaxel, 5-fluorouracil (5-FU), oxaliplatin, and irinotecan; 2) a poly (ADP-ribose) polymerase inhibitor, Olaparib; 3) a cyclin-dependent kinase 4/6 inhibitor, palbociclib; 4) receptor tyrosine kinase inhibitors, including epidermal growth factor receptor (EGFR), platelet-derived growth factor receptor /vascular endothelial growth factor receptor, and phosphoinositide 3-kinase/protein kinase B/mammalian target of rapamycin concordant inhibitors, and 5) multitarget drugs and inhibitors of the proteasome and histone deacetylase (HDAC) (14) (Supplementary Table 3). Live images were obtained using a high-content screening system (Fig. 2A) and cell viability was determined with an ATP monitoring system. The sensitivity to each drug

261 was represented as a clustered heatmap based on the calculated AUC value for each
262 DRC curve (Fig. 2B). The test revealed marked interpatient variability in the PDO
263 response to a single chemotherapy agent (Fig. 2B). Most drugs were not very effective
264 at inducing cell death in PDAC PDOs. One of the preferred chemotherapy regimens
265 for metastatic and locally-advanced PDAC, gemcitabine and nab-paclitaxel,
266 significantly decreased the viability in a dose-dependent manner. In addition,
267 Trametinib (Mitogen-activated protein kinase inhibitor), Triptolide (NRF2 and NF-kB
268 inhibitor), Panobinostat (HDAC inhibitor) and some EGFR inhibitors including
269 AZD9291, Afatinib, Dacomitinib and Neratinib showed some anti-cancer effect against
270 PDAC PDOs even though these drugs have not shown clinical benefit in PDACs.

271 **PDO sensitivity correlates with therapeutic response in patients with PDAC**

272 The drug sensitivity for each drug differed among the twenty PDAC PDOs.
273 Only 15 of 20 patients received chemotherapy in consideration of their performance
274 status; of these, twelve patients were treated with GnP, and three patients were treated
275 with FOLFIRINOX. Sensitive or resistant PDOs were divided by the median value of
276 normalized AUC for each drug. Because we tested each single drug only, not in
277 combination, PDOs were considered sensitive to GnP if they were sensitive to either
278 gemcitabine or nab-paclitaxel. Likewise, PDO was regarded as sensitive to
279 FOLFIRINOX if it was sensitive to any of oxaliplatin, 5-FU and irinotecan. The
280 concordance between the response to chemotherapy according to RECIST v1.1 in
281 patients and the sensitivity of matched PDAC PDOs was estimated to be 86.7 % (13
282 of 15) (Fig. 2C). Fig. 3A shows the different responses to gemcitabine and nab-
283 paclitaxel among PDAC PDOs. The PDO from Patient 15 who were diagnosed with
284 stage IV disease was sensitive to both gemcitabine and nab-paclitaxel (a red spot in

285 Fig. 3A), and showed good prognosis with OS of 31.07 months, showing the best
286 response as partial response (PR) until 15 cycles with the 1st line GnP treatment, and
287 the progression-free survival (PFS) of 20.87 months (Fig. 3B). The PDO from Patient
288 20 diagnosed with stage III disease was resistant to both gemcitabine and nab-
289 paclitaxel (a green spot in Fig. 3A) and the patient showed a poor prognosis with OS
290 of 10.1 months, showing the best response as stable disease (SD) at the third cycle
291 with the 1st line GnP treatment, and PFS of 7.93 months (Fig. 3C). Also, Fig. 3D shows
292 the different responses to FOLFIRINOX among PDAC PDOs. The PDO from Patient
293 11 diagnosed with stage IV disease with liver metastasis showed sensitivity to 5-FU,
294 irinotecan, and oxaliplatin (a blue spot in Fig. 3D). After treatment with the 10th cycle
295 of FOLFIRINOX, the primary pancreatic mass showed a marked decrease in size, and
296 the hepatic metastases nearly disappeared; however, during subsequent
297 chemotherapy, the patient died from neutropenic septic shock with PFS of 7.3 months
298 (Fig. 3E). The PDO from Patient 1 diagnosed with stage IV disease with peritoneal
299 seeding showed resistance to 5-FU, irinotecan, and oxaliplatin (a yellow spot in Fig.
300 3D). After treatment with FOLFIRINOX, rapid and extensive disease progression was
301 observed in the primary mass, hepatic metastases, and newly appeared brain
302 metastases with PFS of 1.4 months (Fig. 3F). Therefore, this indicates a high
303 concordance between the PDO response and the clinical response of the patient with
304 PDAC to the chemotherapeutic drugs.

305 **Expression Profiling of Genes Related to the Response to Chemotherapeutics**

306 To identify genes whose expression levels are associated with the response to
307 nab-paclitaxel, we performed whole-transcriptome sequencing (WTS) analysis of the
308 PDAC PDOs. Differential gene expression analysis identified 127 upregulated and 113

309 downregulated genes in the nab-paclitaxel-resistant PDOs (Supplementary Fig. 5).
310 Hierarchical clustering analysis of the PDAC PDOs based on the DEGs revealed two
311 distinct response groups, which is concordant with our HTS results (Fig. 4A). Gene
312 set enrichment tests of the DEGs revealed that resistant PDOs were significantly
313 enriched in the hematopoietic cell lineage, sphingolipid metabolism, protein digestion
314 and absorption, renin-angiotensin system, ECM-receptor interaction,
315 glycosaminoglycan biosynthesis and riboflavin metabolism (Fig. 4B and
316 Supplementary Table 4). Additionally, the downregulated DEGs were mainly
317 associated with alanine, aspartate, and glutamate metabolism; phenylalanine, tyrosine,
318 and tryptophan biosynthesis; pyrimidine metabolism; and signaling pathways
319 regulating pluripotent stem cells in the KEGG pathway analysis (Fig. 4B and
320 Supplementary Table 5). To further identify whether the upregulated DEGs affect the
321 prognosis of PDAC patients, we conducted a survival analysis in a large cohort (N=178)
322 from TCGA for some genes related to epithelial-mesenchymal transition and
323 metastasis. The high expression levels of *ITGB7* (*P*=0.038), *ANPEP* (*P*=0.017), and
324 *ST3GAL1* (*P*=0.0056) were significantly associated with poor survival in PDAC
325 patients (Fig. 4C). A high expression level of *CSF2* was also marginally related to the
326 prognosis of PDAC patients (*P*=0.068; Fig. 4C). Although there was no significance in
327 our small cohort, the expression of *ST3GAL1, ANPEP*, *ITGB7*, and *CSF2* genes
328 similarly tended to show differences in OS (Supplementary Fig. 6).
329

330 ## Discussion

331 Here, we successfully established PDAC PDOs from minimal EUS-FNB
332 tissues of unresectable PDAC patients, which PDOs were subjected to the HTS drug

sensitivity test in a short period, within one month after diagnosis using our platform. The PDOs were strictly verified through histologic investigation and integrated analysis of genomic profiling. The drug response of the PDAC PDOs was compatible with the patient response to treatment in the real-world. Additionally, it was possible to explore candidate novel biomarkers associated with the prognosis of PDAC patients according to the drug response.

PDAC PDO platforms with EUS-FNB specimens are essential to predict treatment response in a timely manner. Most genomic studies of PDACs are based on surgical specimens representing an early-stage disease (Stage I/II), a minority of the patient population. Recently, Tiriac *et al*. introduced PDAC PDOs from surgical resection specimens and FNBs (10, 11). This platform helps to overcome the long-standing debates on the known weaknesses of cancer organoids. Tissue acquisition through EUS-FNB has been mostly well standardized, and relatively easy to make standard protocol in detail. It guarantees to yield high-purity cancer cells containing no other normal epithelial cells, stromal cells, or blood cells, especially with the Franseen needle used in our center (31, 32). Technically, it is also possible to obtain tissues that are representative of the entire tumor by puncturing the tumor from multiple directions or utilizing fanning techniques with stylet-retraction maneuvers (33). In addition, it is possible to create PDOs by serially obtaining tissues by EUS-FNB at clinically critical points such as before and after chemotherapy or surgery, identifying their changes in characteristics and changes in drug sensitivity according to the disease course, so they can be used as an evolving avatar for personalized treatment (34-36).

Recent studies sought to predict clinical treatment responses and to choose the best treatments for precision medicine based on PDOs (34, 37). The clinical

357 significance of the PDAC PDO model is its role as a predictive avatar model for the
358 actual patient response to treatment. Our HTS platform using PDAC PDOs provides
359 drug response data that considerably reflect the true clinical response to
360 chemotherapy in the real-world. These results were in line with previous studies
361 suggesting the necessity of a personalized approach using tailored medicine in PDAC
362 (10, 12, 38). Remarkably, this platform for generating PDAC PDOs and selecting drugs
363 approximately one month after diagnosis is very promising and powerful because it is
364 compatible with real clinical practice. Although the pathologic diagnosis after EUS-
365 FNB was confirmed within 1-2 weeks, treatment delays may occur for a variety of
366 reasons, including patient-induced causes and the utilization of medical resources. In
367 addition, there has been no concrete evidence of benefits for the survival outcome of
368 a shorter time delay of palliative systemic therapy in advanced PDACs, which indicates
369 that the focus of research attention should be on treatment with more appropriate
370 drugs, rather than on when to start treatment (39, 40). The PDO and HTS platform can
371 be helpful in guiding clinicians in making personalized diagnosis and therapeutic
372 decisions for precision medicine and it might be used as a universal tool that does not
373 hinder the usual practice of diagnosis for most PDAC patients. In the future, this
374 platform will become one of the most pivotal standard techniques for precision
375 medicine. In unresectable cases, this platform can be utilized to recommend the
376 optimal systemic chemotherapy regimen, and for resectable cases, it also provides
377 crucial insights for choosing optimal neoadjuvant or adjuvant therapy in a tailored way.
378 Additionally, for patients who have undergone surgical treatment, this platform can
379 facilitate preparation for appropriate treatment in the event of post-surgical recurrence.
380 Furthermore, if the platform is standardized, it may become feasible to assess the

response to drugs already utilized in treating other types of cancer, or the response to novel drugs, and subsequently apply these results to patients.

However, we did not find a reliable association between the response of PDAC PDOs and the survival outcomes according to the choice of treatment drugs. Although this prospective observational study was conducted in a high-volume tertiary center, the analysis was limited to only a small number of patients having both available HTS and comparable clinical follow-up data. During the chemotherapeutic treatment of unresectable PDAC in South Korea, the 1st line chemotherapy regimens, GnP or FOLFIRINOX, can be determined by age, ECOG performance, comorbidities, physician's preference, and other socioeconomic background of the patient. It happened that few patients treated with FOLFIRINOX were included in the analysis. To compensate for these limitations, we are currently conducting an extended version of this prospective cohort study with a larger number of patients to evaluate whether the HTS results of the PDAC PDO platform can be used to select an optimal therapy in terms of individualized medicine in real practice [ClinicalTrials.gov Identifier: NCT04736043].

Improved drug screening methods are needed to identify the most effective treatments. In this study, we aimed to construct a PDAC PDO platform that could be used to predict treatment response with superior efficiency over simple cell models; the model showed a proper establishment timeline, a timely drug response evaluation window and high concordance with the features of matched original PDAC tissue. This thoroughness guarantees the clinical applicability of the PDAC PDO model as an *in vitro* screening platform to choose the optimal treatment for individual patients. The findings of our study may be relevant to both patients with unresectable cases and to

those with resectable cases requiring systemic therapy.

Declarations

Ethics approval and consent to participate: Ethical approval was obtained from the institutional review board of the Samsung Medical Center (IRB No. 2014-04-061, 2016-05-011).

Consent for publication: All authors consent to the publication of this article.

Availability of data and materials: All data and material during the current study are available from the corresponding author on reasonable request.

Competing interests: The authors declare that they have no known competing financial interests or personal relationships that could have appeared to influence the work reported in this paper.

Funding: This work was supported by the National Research Foundation (NRF) of Korea funded by the Ministry of Science and ICT (MSIT) (Grant No. NRF-2017R1A2B2007130, NRF-2019R1C1C1008646, NRF-2020R1F1A1072692, NRF-2020R1A2C2102023, NRF-2020R1A2C3006535 and NRF-2021R1A2C1094009), and a grant from the Korean Gastroenterology Fund for Future Development. This research was also supported by the Collaborative Genome Program for Fostering New Post-Genome industry through the NRF, funded by the MSIT (Grant No. NRF-2017M3C9A5031002 and NRF-2017M3C9A5031004), the Basic Science Research Program through the NRF funded by the Ministry of Education (Grant No. NRF-2018R1A6A1A03025810), and the Bio & Medical Technology Development Program of the National Research Foundation (NRF) funded by the Korean government (MSIT) (Grant No. NRF-2016M3A9B4918405). This study was also supported by the Future

Medicine 20*30 project of the Samsung Medical Center (SMC) (Gant No. SMX1230041, SMO1230021) and a SMC Research and Development Grant (Gant No. SMO1230661).

Author contributions: HK - analysis and interpretation of the data, drafting of the article, critical revision of the article for important intellectual content; JJ - analysis and interpretation of the data, drafting of the article; JHC - drafting of the article, critical revision of the article for important intellectual content; JHS- analysis and interpretation of the data, drafting of the article; SHL, JP, SKR, EML, H-OJ and SK - analysis and interpretation of the data; S-HL, KHL, KTL, KMK, and K-TJ - conception and design; HL, SL, JKL, and JKP - conception and design, final approval of the article. All authors read and approved the final manuscript.

Acknowledgements: The authors would like to express their great appreciation of the late DJ. Park and HJ. Kim. We believe that their generous donation will make a tremendous difference to the better treatment and survival of such a devastating disease.

453 ## References

454 1. Ryan DP, Hong TS, Bardeesy N. Pancreatic adenocarcinoma. N Engl J Med.
455 2014;371(11):1039-49.
456 2. Siegel RL, Miller KD, Jemal A. Cancer statistics, 2020. CA Cancer J Clin.
457 2020;70(1):7-30.
458 3. Hidalgo M. Pancreatic cancer. N Engl J Med. 2010;362(17):1605-17.
459 4. Conroy T, Desseigne F, Ychou M, Bouche O, Guimbaud R, Becouarn Y, et al.
460 FOLFIRINOX versus gemcitabine for metastatic pancreatic cancer. N Engl J Med.
461 2011;364(19):1817-25.
462 5. Von Hoff DD, Ervin T, Arena FP, Chiorean EG, Infante J, Moore M, et al.
463 Increased survival in pancreatic cancer with nab-paclitaxel plus gemcitabine. N Engl
464 J Med. 2013;369(18):1691-703.
465 6. Drost J, Clevers H. Organoids in cancer research. Nat Rev Cancer.
466 2018;18(7):407-18.
467 7. Huang L, Holtzinger A, Jagan I, BeGora M, Lohse I, Ngai N, et al. Ductal
468 pancreatic cancer modeling and drug screening using human pluripotent stem cell-
469 and patient-derived tumor organoids. Nat Med. 2015;21(11):1364-71.
470 8. Lau HCH, Kranenburg O, Xiao H, Yu J. Organoid models of gastrointestinal
471 cancers in basic and translational research. Nat Rev Gastroenterol Hepatol.
472 2020;17(4):203-22.
473 9. Boj SF, Hwang CI, Baker LA, Chio, II, Engle DD, Corbo V, et al. Organoid
474 models of human and mouse ductal pancreatic cancer. Cell. 2015;160(1-2):324-38.
475 10. Tiriac H, Belleau P, Engle DD, Plenker D, Deschênes A, Somerville TDD, et al.

476 Organoid Profiling Identifies Common Responders to Chemotherapy in Pancreatic
477 Cancer. Cancer Discov. 2018;8(9):1112-29.
478 11. Tiriac H, Bucobo JC, Tzimas D, Grewel S, Lacomb JF, Rowehl LM, et al.
479 Successful creation of pancreatic cancer organoids by means of EUS-guided fine-
480 needle biopsy sampling for personalized cancer treatment. Gastrointest Endosc.
481 2018;87(6):1474-80.
482 12. Driehuis E, van Hoeck A, Moore K, Kolders S, Francies HE, Gulersonmez MC,
483 et al. Pancreatic cancer organoids recapitulate disease and allow personalized drug
484 screening. Proc Natl Acad Sci U S A. 2019;116(52):26580-90.
485 13. Facciorusso A, Crinò SF, Ramai D, Madhu D, Fugazza A, Carrara S, et al.
486 Comparative diagnostic performance of different techniques for EUS-guided fine-
487 needle biopsy sampling of solid pancreatic masses: a network meta-analysis.
488 Gastrointest Endosc. 2023;97(5):839-48.e5.
489 14. Lee JK, Liu Z, Sa JK, Shin S, Wang J, Bordyuh M, et al. Pharmacogenomic
490 landscape of patient-derived tumor cells informs precision oncology therapy. Nat
491 Genet. 2018;50(10):1399-411.
492 15. Li H, Durbin R. Fast and accurate short read alignment with Burrows-Wheeler
493 transform. Bioinformatics (Oxford, England). 2009;25(14):1754-60.
494 16. Cibulskis K, Lawrence MS, Carter SL, Sivachenko A, Jaffe D, Sougnez C, et
495 al. Sensitive detection of somatic point mutations in impure and heterogeneous cancer
496 samples. Nat Biotechnol. 2013;31(3):213-9.
497 17. Boeva V, Popova T, Bleakley K, Chiche P, Cappo J, Schleiermacher G, et al.
498 Control-FREEC: a tool for assessing copy number and allelic content using next-
499 generation sequencing data. Bioinformatics. 2012;28(3):423-5.

500 18. Favero F, Joshi T, Marquard AM, Birkbak NJ, Krzystanek M, Li Q, et al.
501 Sequenza: allele-specific copy number and mutation profiles from tumor sequencing
502 data. Ann Oncol. 2015;26(1):64-70.
503 19. Love MI, Huber W, Anders S. Moderated estimation of fold change and
504 dispersion for RNA-seq data with DESeq2. Genome Biol. 2014;15(12):550.
505 20. Chen EY, Tan CM, Kou Y, Duan Q, Wang Z, Meirelles GV, et al. Enrichr:
506 interactive and collaborative HTML5 gene list enrichment analysis tool. BMC
507 Bioinformatics. 2013;14:128.
508 21. Kuleshov MV, Jones MR, Rouillard AD, Fernandez NF, Duan Q, Wang Z, et al.
509 Enrichr: a comprehensive gene set enrichment analysis web server 2016 update.
510 Nucleic Acids Res. 2016;44(W1):W90-7.
511 22. Baeuerle PA, Gires O. EpCAM (CD326) finding its role in cancer. Br J Cancer.
512 2007;96(3):417-23.
513 23. Karantza V. Keratins in health and cancer: more than mere epithelial cell
514 markers. Oncogene. 2011;30(2):127-38.
515 24. Reichert M, Takano S, Heeg S, Bakir B, Botta GP, Rustgi AK. Isolation, culture
516 and genetic manipulation of mouse pancreatic ductal cells. Nat Protoc.
517 2013;8(7):1354-65.
518 25. Kopp JL, Dubois CL, Schaffer AE, Hao E, Shih HP, Seymour PA, et al. Sox9+
519 ductal cells are multipotent progenitors throughout development but do not produce
520 new endocrine cells in the normal or injured adult pancreas. Development.
521 2011;138(4):653-65.
522 26. Bausch D, Thomas S, Mino-Kenudson M, Fernandez-del CC, Bauer TW,
523 Williams M, et al. Plectin-1 as a novel biomarker for pancreatic cancer. Clin Cancer

524 Res. 2011;17(2):302-9.

525 27. Oshima Y, Suzuki A, Kawashimo K, Ishikawa M, Ohkohchi N, Taniguchi H.
526 Isolation of mouse pancreatic ductal progenitor cells expressing CD133 and c-Met by
527 flow cytometric cell sorting. Gastroenterology. 2007;132(2):720-32.

528 28. Buscail L, Bournet B, Cordelier P. Role of oncogenic KRAS in the diagnosis,
529 prognosis and treatment of pancreatic cancer. Nat Rev Gastroenterol Hepatol.
530 2020;17(3):153-68.

531 29. di Magliano MP, Logsdon CD. Roles for KRAS in pancreatic tumor
532 development and progression. Gastroenterology. 2013;144(6):1220-9.

533 30. Integrated Genomic Characterization of Pancreatic Ductal Adenocarcinoma.
534 Cancer Cell. 2017;32(2):185-203.e13.

535 31. Gkolfakis P, Crinò SF, Tziatzios G, Ramai D, Papaefthymiou A, Papanikolaou
536 IS, et al. Comparative diagnostic performance of end-cutting fine-needle biopsy
537 needles for EUS tissue sampling of solid pancreatic masses: a network meta-analysis.
538 Gastrointestinal endoscopy. 2022;95(6):1067-77.e15.

539 32. Bang JY, Hebert-Magee S, Navaneethan U, Hasan MK, Hawes R,
540 Varadarajulu S. EUS-guided fine needle biopsy of pancreatic masses can yield true
541 histology. Gut. 2018;67(12):2081-4.

542 33. Bang JY, Jhala N, Seth A, Krall K, Navaneethan U, Hawes R, et al.
543 Standardisation of EUS-guided FNB technique for molecular profiling in pancreatic
544 cancer: results of a randomised trial. Gut. 2023;72(7):1255-7.

545 34. Seppälä TT, Zimmerman JW, Suri R, Zlomke H, Ivey GD, Szabolcs A, et al.
546 Precision Medicine in Pancreatic Cancer: Patient-Derived Organoid Pharmacotyping
547 Is a Predictive Biomarker of Clinical Treatment Response. Clinical cancer research :

548 an official journal of the American Association for Cancer Research.
549 2022;28(15):3296-307.
550 35. Hennig A, Baenke F, Klimova A, Drukewitz S, Jahnke B, Brückmann S, et al.
551 Detecting drug resistance in pancreatic cancer organoids guides optimized
552 chemotherapy treatment. The Journal of pathology. 2022;257(5):607-19.
553 36. Farshadi EA, Chang J, Sampadi B, Doukas M, Van 't Land F, van der Sijde F,
554 et al. Organoids Derived from Neoadjuvant FOLFIRINOX Patients Recapitulate
555 Therapy Resistance in Pancreatic Ductal Adenocarcinoma. Clinical cancer research :
556 an official journal of the American Association for Cancer Research.
557 2021;27(23):6602-12.
558 37. Grossman JE, Muthuswamy L, Huang L, Akshinthala D, Perea S, Gonzalez
559 RS, et al. Organoid Sensitivity Correlates with Therapeutic Response in Patients with
560 Pancreatic Cancer. Clinical cancer research : an official journal of the American
561 Association for Cancer Research. 2022;28(4):708-18.
562 38. Bailey P, Chang DK, Nones K, Johns AL, Patch AM, Gingras MC, et al.
563 Genomic analyses identify molecular subtypes of pancreatic cancer. Nature.
564 2016;531(7592):47-52.
565 39. Lee SH, Chang PH, Chen PT, Lu CH, Hung YS, Tsang NM, et al. Association
566 of time interval between cancer diagnosis and initiation of palliative chemotherapy with
567 overall survival in patients with unresectable pancreatic cancer. Cancer medicine.
568 2019;8(7):3471-8.
569 40. Jooste V, Dejardin O, Bouvier V, Arveux P, Maynadie M, Launoy G, et al.
570 Pancreatic cancer: Wait times from presentation to treatment and survival in a
571 population-based study. International journal of cancer. 2016;139(5):1073-80.

Table 1. Baseline characteristics of study patients and analysis of the factors associated with PDAC PDO success

Characteristics		Baseline	Univariate Analysis		Multivariate Analysis	
			OR	p value	OR	p value
Age (years)	median (range)	65 (37-84)	1.00 (0.95-1.05)	0.891		
Gender	Male (%)	65 (57.5)	1	0.141		
	Female (%)	48 (42.5)	0.47 (0.17-1.28)			
BMI (kg/m^2)	median (range)	22.3 (20.3-25.3)	0.95 (0.88-1.04)	0.287		
Smoking	No (%)	77 (68.1)	1	0.274		
	Yes (%)	36 (31.9)	1.94 (0.59-6.32)			
Performance status (ECOG)	0: Fully active	101 (89.4)	1	0.88		
	1: Light housework	9 (8.0)	1.74 (0.20-14.75)	0.614		
	2: Ambulatory	3 (2.7)	1.00 (1.00-1.00)	0.999		
Comorbidity	No (%)	58 (51.3)	1	0.531		
	Yes (%)	55 (48.7)	0.73 (0.27-1.97)			
CEA (ng/mL)	< 5-7 (normal range)	3.1 (1.8-7.4)	1.00 (0.99-1.01)	0.76	1.00 (0.99-1.00)	0.9
CA 19-9 (U/mL)	< 5-7 (normal range)	195.9 (31.2-1722.6)	1.00 (1.00 -1.00)	0.42		
AJCC 8th stage of cancer	I (IA, IB) (%)	14 (12.4)	1	0.478	1	0.479
	II (IIA, IIB) (%)	7 (6.2)	0.46 (0.03-8.69)	0.606	0.84 (0.04-17.46)	0.908
	III (%)	33 (29.2)	0.56 (0.06-5.49)	0.617	0.41 (0.04-4.73)	0.8476
	IV (%)	59 (52.2)	0.27 (0.03-2.28)	0.23	0.23 (0.02-2.33)	0.211
Metastasis	No metastasis (%)	54 (47.8)	1	0.109		
	Liver metastasis (%)	28 (24.8)	0.75 (0.19-2.91)	0.678		
	Other site metastasis, not liver (%)	31 (27.4)	0.31 (0.10-0.96)	0.043		
Location (proximal)	Uncinate or head (%)	57 (50.4)	1	0.181		
	Body (%)	31 (27.4)	0.34 (0.11-1.09)	0.069		
	Tail (%)	25 (22.1)	0.47 (0.13-1.72)	0.254		
Tumor Size (mm)	median (range)	31.0 (25.0-45.0)	0.99 (0.96-1.02)	0.434	0.99 (0.96-1.02)	0.638
Cellularity of specimen	Mild (<3 clusters) (%)	44 (38.9)	1	0.314	1	0.097
	Moderate (3-10 clusters) (%)	34 (30.1)	0.99 (0.33-3.00)	0.988	1.91 (0.41-8.95)	0.413
	High (> 10 clusters) (%)	35 (31.0)	2.74 (0.68-11.03)	0.155	5.60 (1.05-29.93)	0.044
Overall survival (months)	median (range)	15.6 (0.3-69.7)	1.01 (0.97-1.05)	0.629	1.01 (0.96-1.05)	0.775

PDAC, pancreatic ductal adenocarcinoma; PDO, patient-derived organoid; OR, odds ratio; BMI, Body Mass Index; ECOG, Eastern Cooperative Oncology Group; AJCC, the American Joint Committee on Cancer

576 ## Figure legends

577 **Figure 1. Histological and Genomic Concordance between PDAC PDOs and**
578 **primary tumors**

579 **A**. PDOs from PDAC or acute pancreatitis patients and their primary endoscopic
580 ultrasound-guided fine needle biopsy (EUS-FNB) tissues after hematoxylin and eosin
581 (H&E) staining. **B**. Immunofluorescence staining for cytokeratin (CK), EpCAM, DBA-
582 lectin, SOX9, Plectin-1, CD133, and phalloidin to verify PDAC PDOs. **C**. Heatmap
583 displaying the predicted cellularity of each sample and Pearson's correlation
584 coefficient based on the somatic copy number alteration (CAN) profiles between PDO
585 and FNB samples. **D**. Landscape of somatic point mutation profiles in the PDAC PDOs
586 and FNB samples. The number of protein sequence-altering somatic point mutations
587 (single nucleotide variants, SNVs; short insertions and deletions, Indels) are displayed
588 at the top. Frequently mutated genes are listed in decreasing order of their mutation
589 frequency. The percentages of samples with a mutated gene are displayed at the right.

590 **Figure 2. A Platform of High-Throughput Drug Screening using PDAC PDOs**

591 **A**. Pancreatic ductal adenocarcinoma (PDAC) patient-derived organoids (PDOs) were
592 treated with 71 kinds of drugs with 7-point serial dilutions. After 7 days, cell viability
593 was assessed, and images were obtained with a high-content screening (HCS) system.
594 DMSO and PBS were used as negative control, and Bortezomib (1 mM) was used as
595 positive control for drug sensitivity test. **B**. Heatmap of the chemotherapeutic drug
596 response profile of PDAC PDOs based on the AUC value calculated from the high-
597 throughput screening (HTS) drug sensitivity test. Higher AUC (red) means more
598 resistance to drugs, while lower AUC (blue) indicates more sensitivity to drugs. **C**.
599 Heatmap displaying the chemotherapeutic response of PDAC patients and their PDOs.

600 Red and blue colors denote resistance and sensitivity, respectively, of PDOs from the
601 HTS drug sensitivity test. White and grey colors indicate responsive and non-
602 responsive patients, respectively, to chemotherapy in the real-world.

603 **Figure 3. Clinical Correlation of Chemotherapeutic Sensitivity between PDAC**
604 **PDOs and Patients.**

605 **A**. Normalized AUC distribution for gemcitabine and nab-paclitaxel. **B**. Computerized
606 tomography (CT) scan images before and after treatment of a gemcitabine combined
607 with nab-paclitaxel (GnP)-sensitive patient indicated as a red dot in (A). **C**. CT scan
608 image before and after treatment of a GnP-resistant patient indicated as a green dot
609 in (A). **D**. Normalized AUC distribution for 5-fluorouracil (5-FU), irinotecan, and
610 oxaliplatin. **E**. CT scan image before and after treatment of a FOLFIRINOX (5-
611 fluorouracil, leucovorin, irinotecan, and oxaliplatin)-sensitive patient indicated, as a
612 blue dot in (D). **F**. CT scan image before and after treatment of a FOLFIRINOX-
613 resistant patient indicated as a yellow dot in (D).

614 **Figure 4. Transcriptomic/Genomic Profiling of Factors Related to**
615 **Chemotherapeutic Agent Response.**

616 **A**. Heatmap displaying the expression profiles of significant differentially expressed
617 genes (DEGs) between the nab-paclitaxel-resistant and nab-paclitaxel-sensitive
618 PDAC PDOs. Red and blue colors denote z score-normalized high and low expression,
619 respectively, of each gene. Heatmap rows and columns are ordered according to
620 hierarchical clustering. **B**. Bar plots for the results from gene set enrichment analyses
621 of the upregulated (left) and downregulated (right) DEGs between the nab-paclitaxel-
622 resistant and nab-paclitaxel-sensitive PDAC PDO groups using KEGG pathway
623 information. The thresholds for identifying significant DEGs were 1) |log2(Fold

624 Change)| ≥ 1 and 2) *P* value < 0.05. Statistical significance is indicated by the -log (*P*
625 value) on the X-axis, and the enriched pathways are displayed on the Y-axis in
626 decreasing order of -log (*P* value). **C**. Kaplan–Meier (KM) plots displaying the results
627 from survival analysis of TCGA PDAC patients (N=178) according to the expression
628 of ST3GAL1, ANPEP, ITGB7 and CSF2. Log rank *P* values were calculated and are
629 shown in the KM plots.
630
631
632
633
634
635
636
637
638
639
640
641
642
643
644
645
646
647

648 ## Supplementary Legends

649 **Supplementary Figure 1. Workflow of the Study**

650 PDAC tissue specimens obtained by EUS-guided FNB were dissociated mechanically
651 and enzymatically. Dissociated cells were seeded with Matrigel and incubated for the
652 generation of 3-dimensional (3D) PDAC PDOs. PDAC PDOs were stored as stocks
653 (Biobanking), examined by histopathological methods, and treated with
654 chemotherapeutic drugs for viability analysis. DNA/RNA sequencing was performed
655 with primary tumors and their organoids, and clinical information was collected for
656 further integrated analysis.

657 **Supplementary Figure 2. Enrollment of Study Patients**

658 A total of 201 patients with suspected pancreatic ductal adenocarcinoma (PDAC) were
659 enrolled in the study. Among them, 113 patients were diagnosed with PDAC through
660 endoscopic ultrasound-guided fine needle biopsy (EUS-FNB), and 94 PDAC patient-
661 derived organoid (PDO)s were successfully generated. High-throughput screening
662 (HTS) drug sensitivity test was selectively performed with 20 PDAC PDOs.

663 **Supplementary Figure 3.** Kaplan–Meier plot of the overall survival of study patients
664 according to the success rate of PDAC PDO culture.

665 **Supplementary Figure 4.** Representative images of PDAC PDOs. Scale bar, 650 μm.

666 **Supplementary Figure 5**. Volcano plot for the DEGs between nab-paclitaxel-resistant
667 and nab-paclitaxel-sensitive PDAC PDOs. Red and blue dots denote upregulated and
668 downregulated DEGs, respectively, with a P value < 0.05 and a |log2(Fold Change)| ≥
669 1. Red and blue colors denote upregulated and downregulated genes, respectively.

670 **Supplementary Figure 6.** Kaplan–Meier plots displaying the results from the survival
671 analysis of PDAC patients (N=17) according to the expression of ST3GAL1, ANPEP,

672 ITGB7 and CSF2. Log rank *P* values were calculated and are shown in the plots.

673 **Supplementary Video.** Image stacking of a growing 3D PDAC PDO culture from the
674 bottom to the top of Matrigel.

675 **Supplementary Table 1.** Composition of Complete medium for patient-derived
676 organoid culture

677 **Supplementary Table 2.** Antibodies for Immunostaining

678 **Supplementary Table 3.** Drug list and classification

679 **Supplementary Table 4.** Upregulated DEGs in the KEGG pathway analysis

680 **Supplementary Table 5.** Downregulated DEGs in the KEGG pathway analysis

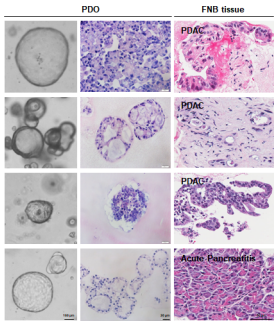

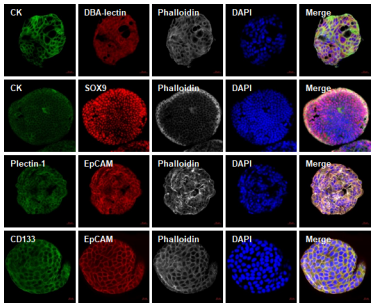

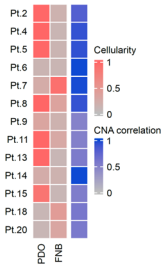

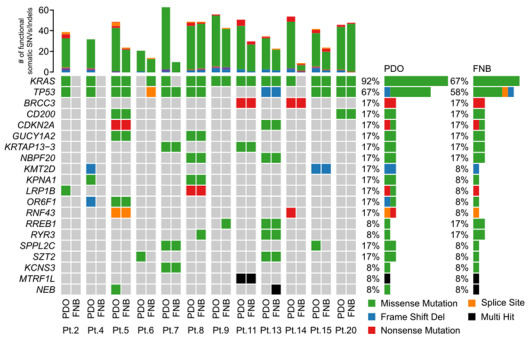

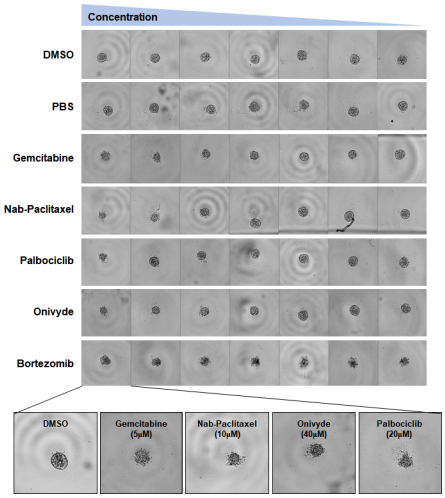

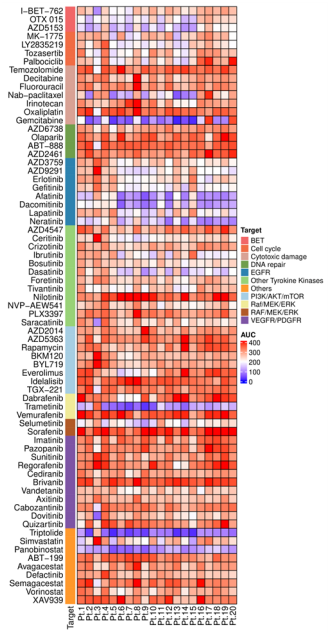

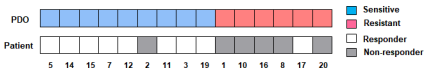

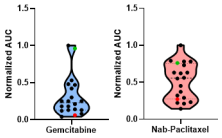

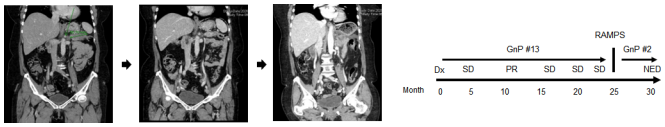

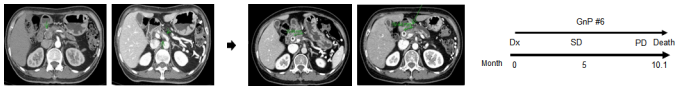

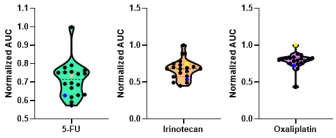

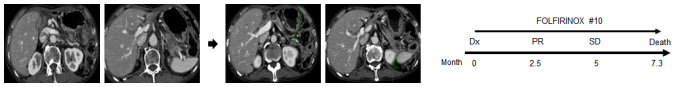

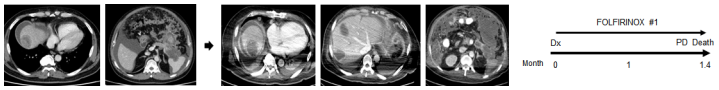

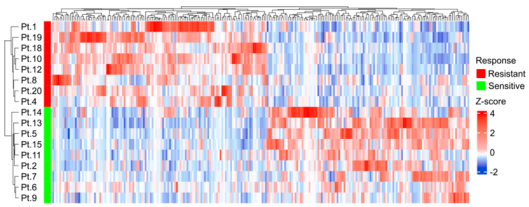

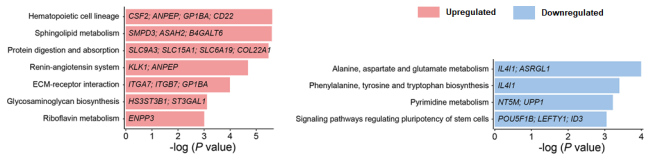

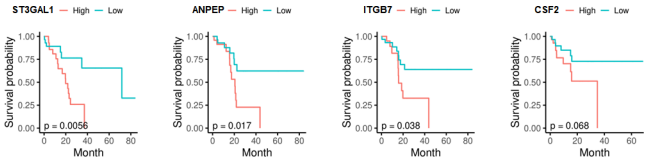

List of abbreviations

PDAC: pancreatic ductal adenocarcinoma

PDO: patient-derived organoid

EUS-FNB: endoscopic ultrasonography-guided fine needle biopsy

HTS: high-throughput screening

FOLFIRINOX: 5-fluorouracil, leucovorin, irinotecan, and oxaliplatin

GnP: gemcitabine and nab-paclitaxel

BMI: body mass index

ECOG: Eastern Cooperative Oncology Group

CEA: serum carcinoembryonic antigen

CA19-9: carbohydrate antigen 19-9

OS: overall survival

DFS: disease-free survival

PR: partial response

SD: stable disease

PD: progressive disease

AJCC: American Joint Committee on Cancer

CK: Cytokeratin

DRC: dose–response curve

AUC: area under the curve

WES: whole-exome sequencing

WTS: whole-transcriptome sequencing

SCNA: somatic copy number alteration

SNV: single nucleotide variation

Indels: insertions and deletions

DEG: differentially expressed gene

TCGA: The Cancer Genome Atlas

KEGG: Kyoto Encyclopedia of Genes and Genomes

GSEA: gene set enrichment test